Mixing and Chaotic Microstructure

Yuefan Deng, James Glimm, and David H. Sharp

Mixing is a process in which distinct fluids intermingle in a complex way. Chaotic microstructure refers, more broadly, to all small-scale stochastic or chaotic behavior that affects dynamics at large length scales. Problems that involve mixing and chaotic microstructure are of fundamental importance in both basic science and engineering: They are the central issue in turbulence, pipeline flow, and the dynamics of supernovae. The microstructure of porous rocks, which is stochastic on all length scales, is a dominant aspect of the geology of aquifers and oil reservoirs. Chaotic microstructure also plays a key role in determining the properties of common materials such as metals and plastics. Mixing is a dominant phenomenon limiting the performance of pellets in laser-fusion experiments.

Without doubt the problem of chaotic microstructure, in its many ramifications, is the most fundamental in classical continuum physics. Why is this? First, because the problem is pervasive, and second because the only systematic solution occurs at the engineering level through the method of conservative overdesign, or experimental trial and error. The classical methods of science—theory, computation, and experiment—have so far delivered much less than is needed either for engineering purposes or for scientific understanding.

These problems are difficult for three reasons. They possess an exceedingly large number of active degrees of freedom, they are usually nonlinear, and they typically do not admit a small parameter for useful expansions. Together these features lead to an extremely complex phenomenology.

We propose here a systematic program for addressing this class of problems. This program follows a line of development that will be familiar to many-body theorists. The first step is the identification and analysis of elementary modes, or coherent structures. For example, in turbulence the elementary modes are vortices; in phase transitions, dendrites; in Hele-Shaw cells, viscous fingers; in solid materials, lattice dislocations. The second step is to understand the pairwise interaction of elementary modes. This step is followed, not by an analysis of multi-mode interactions, but by the

statistical analysis of an ensemble of modes governed by pairwise interactions. From this analysis we want to derive continuum-level constitutive laws (such as equations of state), which are then used (fifth step) in macroscopically averaged flow equations such as the Navier-Stokes equation. Thus we have a five-step procedure relating microscopic dynamics to macroscopic observables. Although each of the steps may seem rather obvious, their integration is less commonly discussed. A large fraction of work in classical physics is related to this program in that it addresses one or another of its steps.

In this paper we will illustrate this program by discussing its implementation in examples drawn from our work and that of our collaborators. This work as well as collateral work of others can be traced from the further reading given at the end of the article.

Rayleigh-Taylor Instability

Our first example concerns Rayleigh-Taylor instability. The occurrence of this instability can be understood in the following simple way. Imagine the ceiling of a room plastered uniformly with water to a depth of 1 meter (Figure 1). The layer of water will fall. However, it is not through lack of support from the air that the water falls. The pressure of the atmosphere is equivalent to that of a layer of water 10 meters thick, quite sufficient to hold the water against the ceiling. But in one respect the atmosphere fails as a supporting medium. It fails to constrain the air-water interface to flatness. No matter how carefully the water layer was prepared, small irregularities are inevitably present at the interface. Those portions of the fluid at the interface that lie higher than the average experience more pressure than is necessary for their support. They begin to rise, pushing aside water as they do so. Neighboring portions of the fluid, where the surface hangs a little lower than average, require more than average pressure for their support. They begin to fall. The air cannot supply the specific variations in pressure from place to place necessary to prevent the interface irregularities from growing. The initial irregularities therefore increase in magnitude, exponentially in time at the beginning. The water falls to the floor.

The same layer of water lying on the floor would have been perfectly stable. Irregularities die out. Thus we can infer a simple criterion for the onset of Rayleigh-Taylor instability at the interface between two fluids of different densities: *If the heavy fluid pushes the light fluid, the interface is stable. If the light fluid pushes the heavy fluid, the interface is unstable.*

Rayleigh-Taylor instability occurs in diverse situations. Let us take a quick look at one example from research into inertial-confinement fusion. Figure 2 shows a highly schematic picture of the implosion of a deuterium-tritium (DT) pellet. A spherical glass or metal tamper is filled with DT gas. The tamper is irradiated with intense laser light, which causes it to accelerate inward, compressing the DT gas inside the cavity in order to bring about nuclear fusion. During irradiation the outer surface of the tamper is the interface between a heavy fluid (glass or metal) and a light fluid (vaporized glass or metal) and is unstable during the initial phase of the implosion, when the light fluid pushes the heavy fluid. As the pellet is compressed to perhaps 1000 times its normal density, the pressure in the cavity increases until it is sufficient

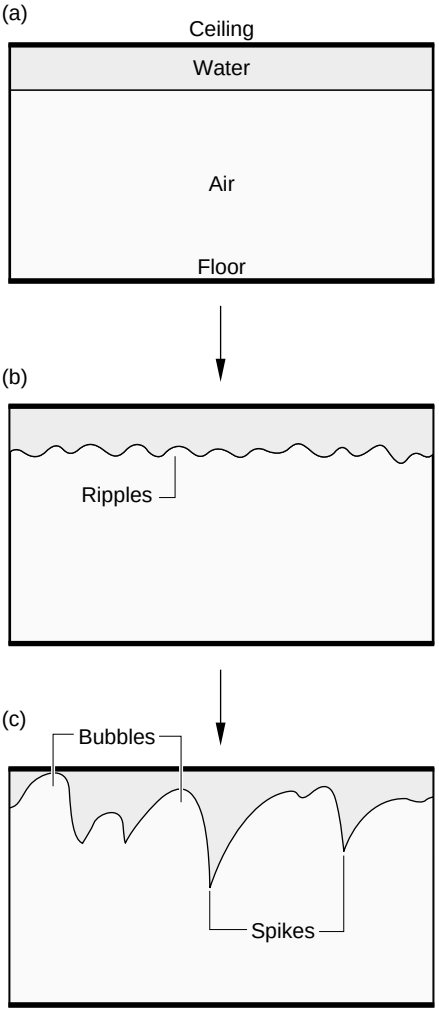

Figure 1. An Example of Rayleigh-Taylor Instability
(a) The pressure of the air is quite sufficient to support a perfectly uniform layer of water 1 meter thick against the ceiling. (b) But the air pressure cannot constrain the air-water interface to flatness. Ripples or irregularites will inevitably be present at the interface. (c) The irregularities grow, forming “bubbles” and “spikes.” The water falls to the floor.

to slow the inward motion of the tamper. This phase of the implosion is also Rayleigh-Taylor unstable; here the high-pressure light gas in the cavity is pushing the tamper. Although this picture of the implosion of a DT pellet is oversimplified in a number of ways, it nevertheless suggests quite clearly that Rayleigh-Taylor instability can have an important effect on the compression of the pellet.

A closer look at the time evolution of a Rayleigh-Taylor unstable interface reveals a complex phenomenology. As the instabilities develop, bubbles of light fluid and spikes of heavy fluid form, each penetrating into the other phase. Complex interactions among bubbles and spikes lead to the formation of a chaotic mixing layer at the interface. Understanding the growth rate and structure of this mixing layer is the central problem in the study of Rayleigh-Taylor instability.

This question has been investigated experimentally by Read and Youngs. Their important findings bring the questions to be understood into sharp focus and can be summarized as follows. The mixing layer has three principal regions: the edge where bubbles of light fluid are penetrating into the heavy fluid (bubble regime), the edge where spikes of heavy fluid are penetrating into the light fluid (spike regime), and the connecting interior region (mixing layer). The bubble regime has been the most carefully studied and has the simplest properties. It is found in the Read and Youngs experiments, as well as in numerical simulations (Figure 3), that the edge of the mixing layer in the bubble regime is dominated by a collection of bubbles.

The average height of the bubbles relative to the mean position of the interface, $h(t)$, grows with time according to the scaling law

$$h(t) = \alpha A g t^2,$$

where A, the Atwood number, is a modification due to buoyancy of the acceleration force (gravity) g and is defined as $A = (\rho_2 - \rho_1)/(\rho_2 + \rho_1)$ in which ρ_i represents the density of fluid i. It is a remarkable experimental finding of Read and Youngs that for incompressible fluids the acceleration constant α in this equation is an approximately *universal* constant, in that it is nearly independent of initial conditions and of fluid properties such as density, viscosity, and surface tension. Finally, it is observed that the average number of bubbles at the interface decreases with time, and that their average radius increases.

The main objective of our work has been to understand the physical properties of the Rayleigh-Taylor mixing layer. The fluid in the mixing layer is in a chaotic state, and it is necessary to have a strategy to guide one through the complexities of this problem. The fundamental challenge in modeling fluid chaos is to provide a simple macroscopic description of a chaotic fluid state that expresses a statistical average of information describing its chaotic microstructure. For the case of chaotic microstruc-

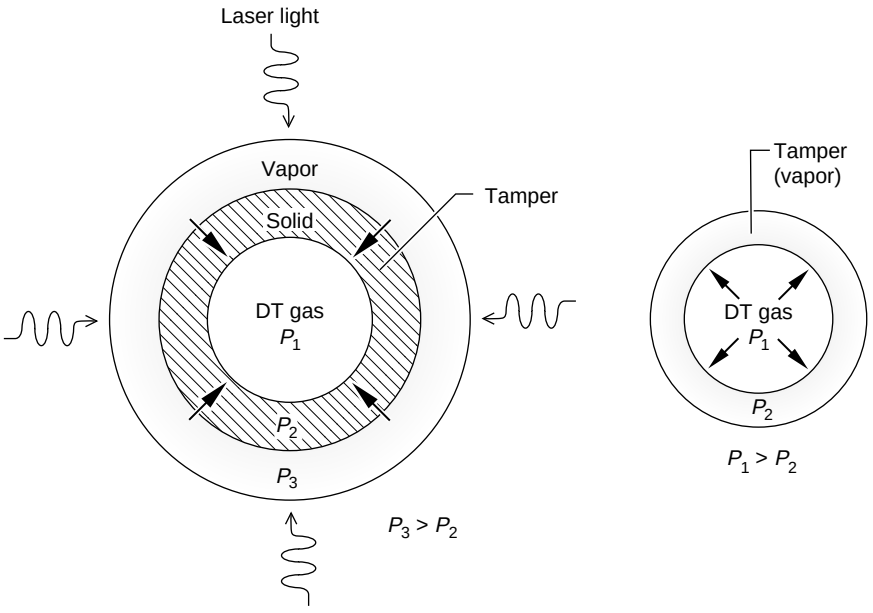

Figure 2. Rayleigh-Taylor Instabilities in Laser Fusion
On the left appears an extremely simplified view of a laser-fusion pellet at an early stage of a fusion experiment. Laser irradiation of the solid tamper vaporizes the outer layer of the tamper and pushes the tamper inward. Because the light vapor is pushing the heavier solid, this stage of the process is Rayleigh-Taylor unstable. On the right is sketched the same experiment at a later stage. Here the DT gas, now at high pressure (P_1), slows the inward motion of the tamper. Since the DT gas is less dense than the tamper, this stage of the process is also Rayleigh-Taylor unstable.

ture at the molecular level, the solution to this problem is highly developed and has given rise to the subjects of thermodynamics and statistical physics to describe the macro- and microphysics respectively.

Adapting the statistical-physics viewpoint to the analysis of fluid chaos,we proceed to study the one- and two-body problems and follow this with an analysis of a statistical ensemble. A renormalization-group fixed point emerges as a simple description of this ensemble.

In molecular physics the elementary modes, or units of analysis, are atoms or molecules. We identify bubbles as the fundamental modes governing the microphysics at one edge of the Rayleigh-Taylor mixing zone. The one-body problem concerns the dynamics of a single bubble. A relatively complete theory of the motion of a single bubble has been developed, which is valid for both compressible and incompressible fluids and includes a formula for the bubble velocity as a function of mode amplitude. This formula contains a small number of parameters, which have been fixed on the basis of analytic formulae, numerical computations, and experiments on periodic arrays of bubbles.

When more than one bubble is present, the bubbles interact. The interactions have a pronounced effect on the behavior of bubbles. The first effect, observed in both experiments and simulations, is that the velocity of a single bubble in a chaotic array of bubbles is typically a factor of 2 greater than that predicted by the single-bubble theory. This is a rather surprising result, which can be understood as follows. In a chaotic array of bubbles, a given bubble has left and right neighbors which generally differ in height and radius. We draw an envelope through the tips of adjacent bubbles. The envelope defines a long-wavelength collective excitation of the fluid and has the appearance of a set of broader bubbles and spikes. These broader bubbles can be viewed as additional elementary modes, which themselves obey the single-bubble theory. Both experiment and simulation led us to the assumption that, although each fundamental bubble is in a deeply nonlinear regime, the interaction of such a bubble with the collective mode is linear, so that the net velocity of a bubble in a chaotic array is given by a simple superposition:

$$v = v_b + v_e,$$

where v_b is the velocity of a bubble of the same amplitude as given by the single-bubble theory, and v_e is the velocity of a bubble in the envelope. The resulting formula agrees very well with experiment; note that it contains *no* free parameters.

The superposition hypothesis captures only one aspect of bubble interactions. The other is bubble merger. Merger refers to the behavior of a pair of neighboring bubbles: a larger, advanced, faster-moving bubble and a smaller, less advanced, slower-moving bubble. (Since larger bubbles move faster, eventually they are always more advanced than smaller bubbles.) It is observed that the smaller bubble is rapidly washed downstream, while the larger bubble increases in size to occupy the portion of the interface vacated by the smaller bubble. Thus, the dynamics of the fundamental modes comprises the dynamics of a single nonlinear

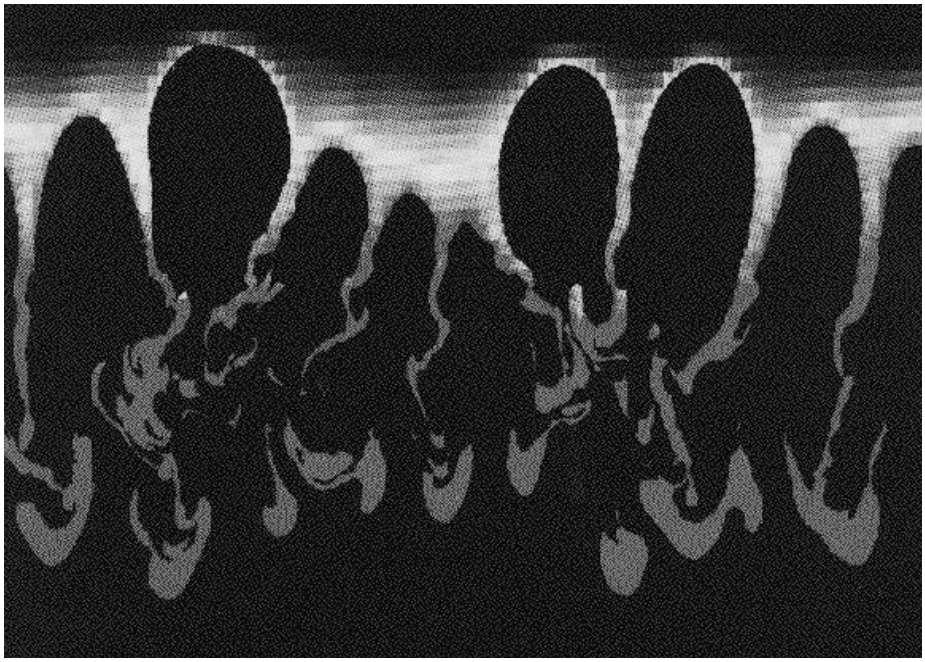

Figure 3. A Simulation of Rayleigh-Taylor Mixing
The figure shows the late-time behavior of Rayleigh-Taylor instability. The dimensionless compressibility $M^2 = 0.5$. The simulation was performed on a 32-node parallel iPSC/860 computer.

mode (single bubble) plus an approximately linear mode-mode velocity coupling plus a highly nonlinear mode-merger process.

We next consider a statistical ensemble of interacting modes (bubbles). We suppose there is a probability distribution for an infinite collection of bubbles, which defines the single-particle distribution (the probability of picking a bubble of height h from the ensemble), the pair correlations, and so forth. The bubble dynamics outlined above defines an evolution in this statistical ensemble of modes. Although the full statistical model could be solved numerically, we instead introduce simplifying assumptions to arrive at a more tractable form of the model. As when the Boltzmann equation is derived in statistical mechanics, we neglect pair correlations; then the probability measure defining the statistical ensemble is determined by the single-particle distributions. Those distributions in turn are approximated in terms of just three time-dependent parameters: the average height of the bubbles, $h(t)$, the variance in bubble height, æ (t), and the bubble radius, $r(t)$. The bubble dynamics leads to a set of ordinary differential equations for these quantities.

The bubble dynamics can be understood from the perspective of the renomalization-group method. This method has two key steps: "coarse-graining" and "rescaling." The bubble-merger process accomplishes a dynamical coarse-graining of the dynamics, because sets of smaller bubbles are replaced by larger bubbles, without changing the physics. The differential equations for the bubble dynamics thus reflect the coarse-graining of the merger process, as well as a dynamic increase in the length scale of the instability. The next step is to introduce rescaled variables, which subtract out these changing length scales. Once this is done, the result is a renormalization-group equation.

Analysis of this equation revealed the existence of a non-trivial renormalization-group fixed point. This means that the equations have the property that, no matter what the initial values of the variables are, they approach the same asymptotic values, or fixed point. At this fixed point, the width of the mixing layer grows at a constant acceleration, Æ . The theory provides a zero-parameter determination of Æ , which turns out to be in remarkable agreement with experiment. Since Æ is determined by a fixed point, its insensitivity to initial conditions is also explained. Thus our analysis has shown that the main properties of the bubble-dominated part of the chaotic mixing layer are direct consequences of scaling and the existence of a renormalization-group fixed point.

We emphasize that our program has depended in an absolutely essential way on numerical simulation of the solutions of the full two-dimensional, two-fluid Euler equations. These calculations were used in a variety of ways. Calculations of the evolution of Rayleigh-Taylor instability at a random interface were used as a model-independent way to calculate the magnitude of Æ , as well as to establish the insensitivity of Æ to a wider range of initial conditions than were explored experimentally and in a way that was not tied to possible idiosyncrasies of the experimental apparatus. Numerical simulations were used to define parameters in our single-bubble model. They were also used to establish the approximate validity of the modeling assumptions employed to understand bubble interactions and to identify conditions where those assumptions were not valid.

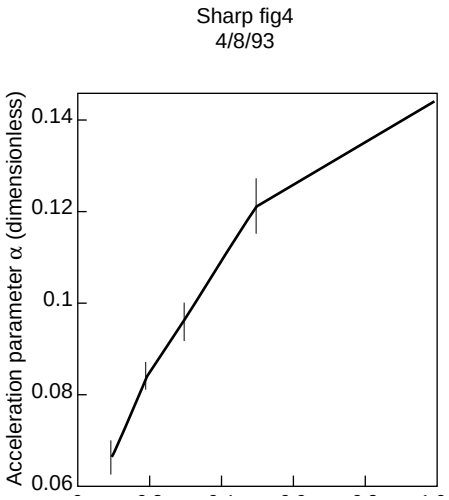

Figure 4. Dependence of the Mixing-Layer Growth Rate on Compressibility
Plot of the growth rate Æ versus the compressibility, M^2. The vertical bars indicate the variance associated with the choice of random-number seed.

Our numerical simulations of Rayleigh-Taylor mixing employed a front-tracking method. Front-tracking works by "hard-wiring" into the code maximal information about the analytically known behavior of the solution near a discontinuity or front (such as the jump in density at the heavy/light interface in the Rayleigh-Taylor problem or at a shock front in gas-dynamics problems). This approach leads to two benefits as well as a cost. The first benefit is the scientific understanding about the behavior of the solution near a discontinuity, generated in the course of implementing the method. The second benefit is that highly accurate solutions can be achieved without recourse to very

fine computational grids. In fact, the front-tracking method typically allows an increase in computational resolution by a factor of about 3.5 in each spatial dimension and in time, that is, by a factor of about 40 in a two-dimensional, time-dependent problem and 150 in a three-dimensional, time-dependent problem. This dramatic increase in efficiency allowed a corresponding increase in the detail and scope of the computations attempted and was instrumental to the success of the program. The cost is that code development for front-tracking is more demanding because more complex algorithms are required to express the information about solution discontinuities. This is basically a software-complexity issue, which has been dealt with by the construction of highly modular code, the use of more powerful programming languages, and other modern code-development methods.

The Read-Youngs experiments were carried out with nearly incompressible fluids. Both our simulation methods and our model apply also to more compressible fluids. It is thus possible to explore, and indeed for the first time to predict, the properties of a chaotic mixing layer in a parameter regime outside the range of existing experiments. Our analysis shows that the mixing-layer growth rate in a compressible fluid can be a factor of 2 larger than in incompressible fluids (see Figure 4), and that Æ develops a dependence on initial conditions. The importance of these results in various applications seems clear.

The final step in our program for the study of high-dimensional chaos is to study continuum-level constitutive laws and equations. Here the flow is regarded as stochastic and flow variables $\Omega = \langle\Omega\rangle + \pm\Omega$, $v = \langle v\rangle + \pm v$, etc., are expressed as sums of mean quantities $\langle\Omega\rangle$, $\langle v\rangle$, etc., and fluctuating quantities $\pm\Omega$, $\pm v$, etc. An effort to write governing equations directly for mean quantities such as $\langle\Omega\rangle$ fails due to the nonlinearity of the governing equations and the fact that the average of a product is not equal to the product of the averages. For this reason, the averaged conservation laws contain new quantities, such as the Reynolds stress:

$$R_{ij} = \langle \rho v_i v_j \rangle - \frac{\langle \rho v_i \rangle \langle \rho v_j \rangle}{\langle \rho \rangle}.$$

The continuum equations, even after quantities such as R_{ij} are introduced as new unknowns with their own dynamical equations, require the introduction of further new quantities (do not close). This means that further modeling assumptions must be made in order to arrive at a complete system of equations. We view these modeling relations as an extension of thermodynamics. Our work in progress in the area is to evaluate the correctness of different modeling approaches. One step in this program is to understand the structure of the fluctuating flow moments, such as R_{ij}, in a Rayleigh-Taylor unstable flow.

Flow in Porous Media

In the example of Rayleigh-Taylor instability discussed above, multiple-length-scale chaos arises spontaneously in a nonlinear dynamical problem. We now turn to an example in which chaos is forced, through the influence of multiple-length-scale data in the definition of the problem. This example concerns the transport and dispersion of pollutants (solutes) in groundwater. There is a nontrivial linear version of this problem, and in this sense it is simpler than the Rayleigh-Taylor problem. The fundamental methodology again consists of the integration of field observations, theory, and computation, but the linearity permits the specialization of the full arsenal of techniques described above and a more complete analysis of the problem. In particular, since the modes in a linear problem do not interact with each other, the study of mode-mode interactions is unnecessary.

As Einstein recognized, the phenomenon of dispersion (the spread of one medium through another) is the macroscopic consequence of random microscopic events. The classical theory of dispersion, based on the assumption that the random events occur on a much shorter scale than the macroscopic observations, leads to the familiar relation

$$l(t) = O(t^{1/2}),$$

where l is the position of the dispersion front and t is time. Field data for transport of fluids through porous media do not satisfy this simple relationship. Porous media of practical interest are heterogeneous on all length scales owing to random variations in the geology. Thus the scale on which the randomness operates is not small relative to the observations, and the assumptions underlying the classical theory of dispersion are not valid. This creates a serious problem for practical engineering in hydrology and in environmental studies of contaminants dispersing in groundwater, for example. In fact there is no known body of knowledge to connect laboratory and field-scale values of dispersivity. Therefore in practice, dispersivity

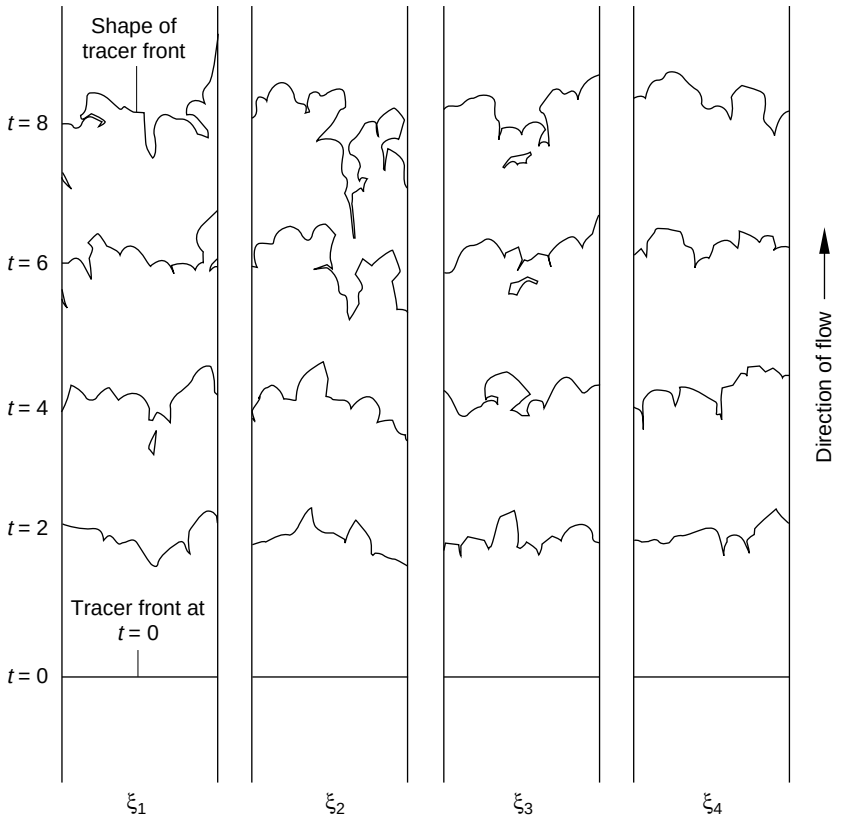

Figure 5. Simulation of Flow through a Porous Medium
Depicted are positions of a tracer front in a fluid flowing through a porous medium. The front is shown at five times (t = 0, 2, 4, 6, 8) for each of four independent simulations. Each simulation uses a different realization of the ^{a} field drawn from a statistical ensemble of geologies.

must be estimated conservatively from carefully instrumented field studies conducted at some other site but at comparable length scales.

Flow through porous media is controlled by unknown (and, at necessary fine scales of detail, unknowable) features of the geological medium such as its porosity. In our studies, we treat those features as random fields, that is, random variables defined at every point of the media. The transmissibility Π is the most important variable relating the geology to flow properties. In analogy to electrical conductivity, it is an inverse resistivity for the flow in the sense that the flow rate equals Π times the negative pressure gradient. We make the common assumption that $\Pi = \exp{}^{a}$, where ^{a} is a normally distributed, random field that depends on the position $\mathbf{x}$ in space and represents the random variations in the structure of the porous medium.

Assuming stationary statistics for simplicity and denoting the ensemble average with angle brackets, we note that $\langle {}^{a}(\mathbf{x})\rangle$ is independent of $\mathbf{x}$ and can be normalized to be zero, so that the entire statistical variation of the flow is determined by the two-point correlation function $\langle {}^{a}(\mathbf{x}){}^{a}(\mathbf{y})\rangle$, which is then a function of the difference variable $\mathbf{x}-\mathbf{y}$; that is, $\langle {}^{a}(\mathbf{x}){}^{a}(\mathbf{y})\rangle = f(\mathbf{x}-\mathbf{y})$. Any choice of f defines a model of the stochastic structure of the rock. A common choice, $f = b\exp(-|\mathbf{x}-\mathbf{y}|/l)$, has a single correlation length scale, l, and thus does not represent variability on all length scales. The simplest form of f that does allow variability on all length scales is the scale-invariant function

$$f = b|\mathbf{x}-\mathbf{y}|^{-\alpha}$$

with $\alpha > 0$. Such a scale-invariant, or self-similar, function is known as a fractal. Somewhat greater generality is obtained by allowing α to be a slowly varying function of $|\mathbf{x}-\mathbf{y}|$.

Randomly varying porous structure (that is, the specification of a ^{a} field) introduces a statistical aspect to the flow. In Figure 5 we plot successive positions of a tracer front (an interface between one part of the fluid, which has been marked with a dye or in some other way, and the rest of the fluid) in four simulations. The simulations used the same initial configuration of the tracer front but different realizations of the ^{a} field, each drawn from the same statistical ensemble of geologies. The statistical variation between the simulations arises, not from a lack of determinism of the flow, but from unpredictability of the flow due to unknown details of the geology. To illustrate this idea, we consider the simplest flow problem: transport of a passive concentration sample of an impurity by a background flow through porous rock. The flow uncertainty would be observable partly as an uncertainty of arrival times of

a concentration sample and partly in the spreading of the concentration gradient due to differing arrival times of the individual particles that compose it. Apart from the rather small effect of molecular mixing on length scales typically of interest, these two aspects of flow uncertainty are identical because the structure of the rock is heterogeneous on all length scales and consequently affects the flow on all scales. The distinction between the two types of uncertainty lies in the resolving ability of the measuring instrument, the size or volume of the initial concentration profile, its initial concentration gradient, and the distance of travel before measurement occurs.

We use dispersion to represent both aspects of uncertainty described above. We can study this dispersion mathematically in terms of the expected values $\langle c(\mathbf{x},t)\rangle$ of a concentration c. The fluctuations, $\pm c = c - \langle c\rangle$, and higher moments such as the covariance, $\langle \pm c \pm c\rangle$, are of interest as well. Similarly, the flow velocity v can be expressed as the sum of its mean and its fluctuating parts: $v = \langle v\rangle + \pm v$. At this point, the flow problem is similar to the transport of a concentration by a turbulent velocity field, such as a pollutant in the atmosphere.

The following methods are available for this class of problems: numerical simulation of the transport process, followed by an ensemble average, to determine $\langle c\rangle$ directly; perturbative solutions of the transport equations in powers of $\pm v$, including resummation methods such as renormalized perturbation theory; analysis of field data; and exact solution of simplified model problems. These methods lead to consistent results and show anomalous (that is, nonclassical) dispersion. This means that the mixing length $l(t)$ associated with the concentration profile $\langle c(\mathbf{x},t)\rangle$ grows in time more rapidly than $t^{1/2}$. When the geology is fractal, $l(t)$ has a fractal behavior as well in the limit of long time, namely,

$$l(t) \propto O(t^{\infty}),$$

and ∞ can be related to the fractal exponent $\emptyset$ of the geology:

$$= \max\left(\frac{1}{2}; 1 - \frac{\emptyset}{2}\right)$$

for $\emptyset > 0$. However, $l(t)$ at short and intermediate times deviates from this law and in fact at short times is fractal with a different exponent.

In contrast to many problems of turbulent mixing, the different methods give consistent results. As Figure 6 shows, perturbative and numerical solutions agree quantitatively, simple soluble models agree asymptotically at long times, and each is consistent with geological field data. However, each of these

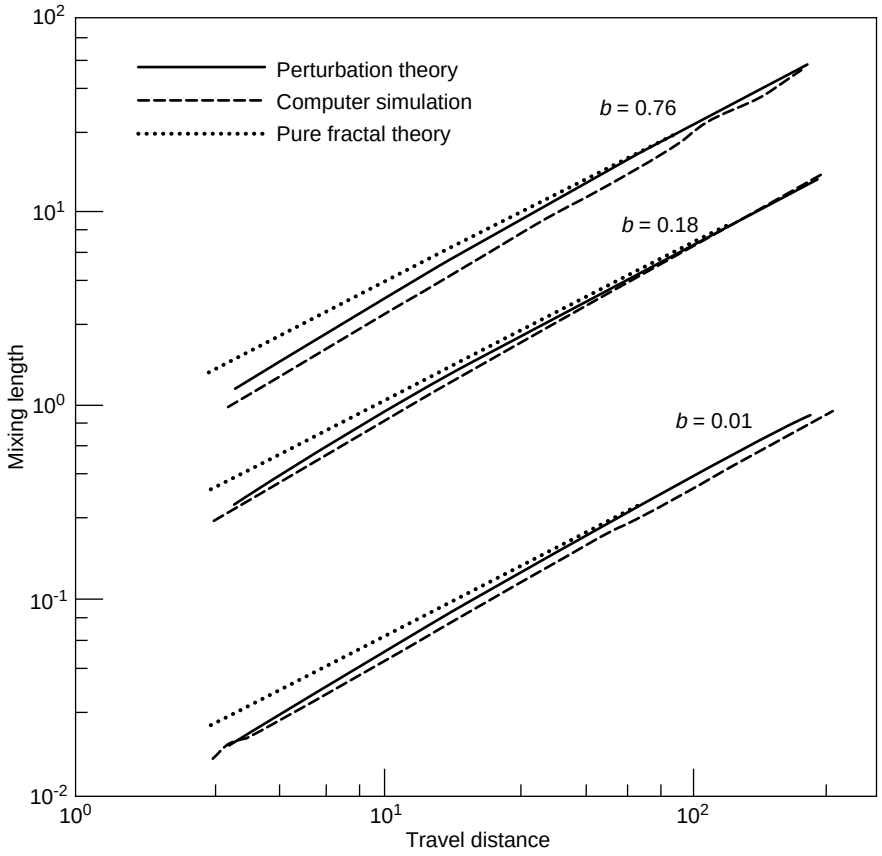

Figure 6. Three Calculations of the Mixing Length in a Porous Medium
The figure is a log-log plot of mixing length, l, as a function of travel distance in a medium having $\emptyset = 0.5$, where $\emptyset$ is the fractal exponent characterizing the stochastic structure of the rock. Each triple of curves shows a comparison between pure fractal theory, second-order transport perturbation theory including transients, and a numerical simulation. Each triple of curves corresponds to a different value of the permeability field coefficient variation, as labeled.

methods is at variance with the results of classical diffusion theory, with a fixed diffusion constant.

Our conclusion is that for geology with unknown fine-scale heterogeneity, dispersion of contaminants in groundwater should depend on time or travel distance, with transient corrections to fractal asymptotics. The understanding of dispersivity and its relation to multiscale geological heterogeneities is important because dispersivity is an essential input into large-scale computational modeling of groundwater-remediation projects. ■

Further Reading

Y. Chen, Y., Deng, J. Glimm, G. Li, D. H. Sharp, and Q. Zhang. A renormalization group scaling analysis for compressible two-phase flow. University at Stony Brook Preprint SUNYSB-AMS-92-02. Submitted to *Physics of Fluids A*

F. Furtado, J. Glimm, W. B. Lindquist, F. Pereira, and Q. Zhang. 1992. Time dependent anomalous diffusion for flow in multi-fractal porous media. In *Proceedings of the Workshop on Numverical Methods for the Simulation of Multiphase and Complex Flow*, edited by T. M. M. Verheggan. New York: Springer Verlag.

J. Glimm, Q. Zhang, and D. H. Sharp. 1991. The renormalization group dynamics of chaotic mixing of unstable interfaces. *Physics of Fluids A* 3: 1333–1335.

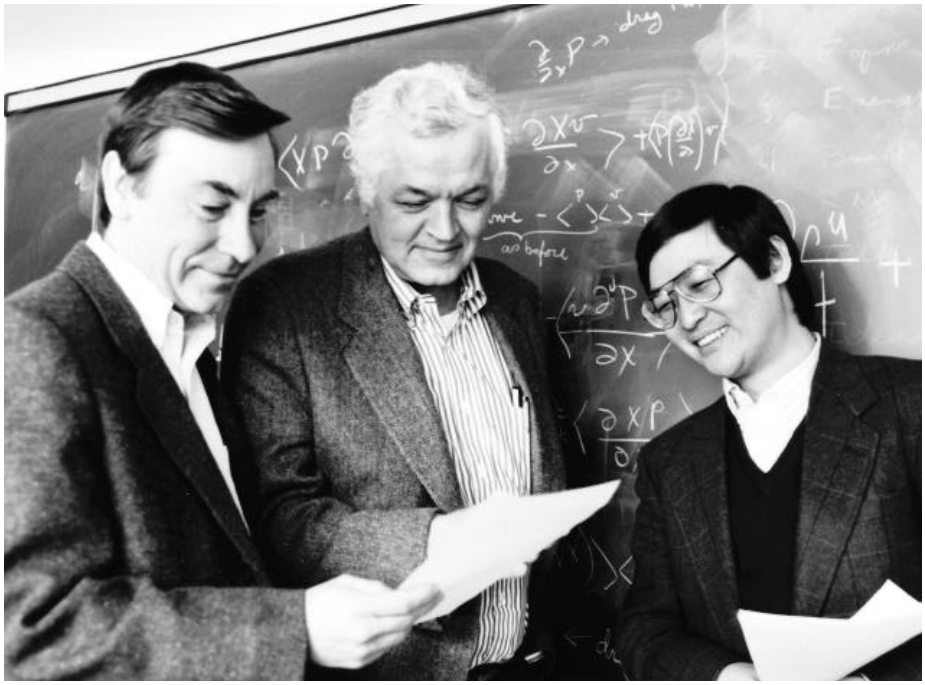

Yuefan Deng (right) was admitted to Columbia University after passing a China-U.S. joint examination and received a Ph. D. in theoretical physics in 1989. He is now an assistant professor in the Department of Applied Mathematics and Statistics at the University at Stony Brook. His main interests include parallel processing and its application to large-scale scientific and engineering problems such as the modeling of multiphase flows, electromagnetic scattering, lattice QCD, and protein folding. His "extra-curricular" activities include writing in Chinese and fixing broken electronic devices.

James Glimm (center) is Chair of the Department of Applied Mathematics and Statistics and Director of the Center for Advanced Manufacturing, both of the University at Stony Brook. He previously held faculty positions at New York University, Rockefeller University, and the Massachusetts Institute of Technology. He is a member of the National Academy of Sciences and recently received the Steele prize of the American Mathematical Society. He has long been interested in DOE problems and visits the Laboratory periodically. His research interests include computation and modeling for turbulent flows, the mathematical theory of conservation laws, and stochastic methods. He enjoys listening to operas and hiking in the mountains.

David H. Sharp (left) received an A.B. from Princeton University in 1960 and a Ph.D. in theoretical physics from the California Institute of Technology. He joined Los Alamos National Laboratory in 1974 and currently holds the position of Laboratory Fellow. Sharp's current research interests include the modeling of complex fluid flows and the formulation and analysis of models of gene regulation. He is a Fellow of the American Association for the Advancement of Science and the American Physical Society.